FULL PAPER

# Exploring the conversion of a D-sialic acid aldolase into a L-KDO aldolase

Adrian Romero-Rivera,[a] Javier Iglesias-Fernández,*[a] and Sílvia Osuna*[a,b]

**Abstract:** Directed evolution involves iterative rounds of genetic diversification followed by selection of variants with improved enzyme properties. A common trend in these studies is the introduction of multiple scattered mutations remote from the active site. Rationalizing how distal mutations influence the conformational states or ensemble of conformations formed by enzymes, and its relation to enzymatic catalysis is highly appealing for the improvement of current rational enzyme design strategies. Directed evolution was applied to convert D-sialic acid aldolase into an efficient L-3-deoxy-manno-2-octulosonic acid (L-KDO) aldolase. In this study, we computationally evaluate the conformational dynamics of both enzymes to shed light on the specificity of the evolved variant. We further demonstrate the role of distal mutations on the modulation of enzyme conformational dynamics and its relation to substrate accessibility and selectivity. Mutations markedly altered active site shape and substrate access tunnels in the evolved L-KDO aldolase, thus affecting the enzyme specificity.

## Introduction

Carbon-carbon bond formation or cleavage is one of the most fundamental reactions in organic chemistry and biology. Aldolase enzymes are found in many pathways of central and secondary metabolism, which catalyze the addition of a ketone to an aldehyde to form a new carbon-carbon bond. Their ability to perform the reaction under mild conditions with high stereoselectivity makes aldolases of extreme value for chemical synthesis.[1] Many protein engineering efforts have been devoted to improve the activity, reverse selectivity and broaden the substrate scope of aldolase enzymes,[1a, 2] and even man-made (retro)-aldolases have been designed by means of semi-rational strategies combining computational enzyme design protocols and Directed Evolution (DE).[3]

D-sialic acid (N-acetyl-D-neuraminic acid) aldolase catalyzes the reversible aldol reaction of N-acetyl-D-mannosamine (ManNAc) and pyruvate to produce D-sialic acid (see Scheme 1). The enzyme is a Class I aldolase that follows an ordered sequential Bi-Uni kinetic mechanism: it first binds pyruvate to form an enamine Schiff-base intermediate (**2**), followed by ManNAc binding to yield the imine Schiff-base intermediate (**4**), that after hydrolysis releases D-sialic acid product (see Scheme 1).[4]

D-sialic acid aldolase features a catalytic Lys165 responsible for the Schiff-base formation with the substrates, and a catalytic triad composed by Tyr137 and Ser47 from one monomeric unit, and Tyr110 from a second subunit. QM/MM-MD simulations together with site-directed mutagenesis confirmed the key role of Tyr137 to act as a proton donor to the aldehyde oxygen of ManNAc for carbon-carbon formation.[4b] Mutation of Ser47 to alanine or cysteine that disrupts the hydrogen bonding network was found to be detrimental for catalysis, whereas the steric bulk of position 110 was crucial for maintaining Ser47 close to Tyr137 for stabilizing its deprotonated form after catalysis.[4b] The study of the reaction mechanism showed that the carbon-carbon bond formation step presents an activation barrier of *ca.* 6-7 kcal/mol when Tyr137, Ser47, and Tyr110 maintain the catalytically competent hydrogen bond network.[4b] QM/MM-MD simulations also suggested that ManNAc binding mode is the main contributing factor to the high stereoselectivity of the enzyme.[4b, 5]

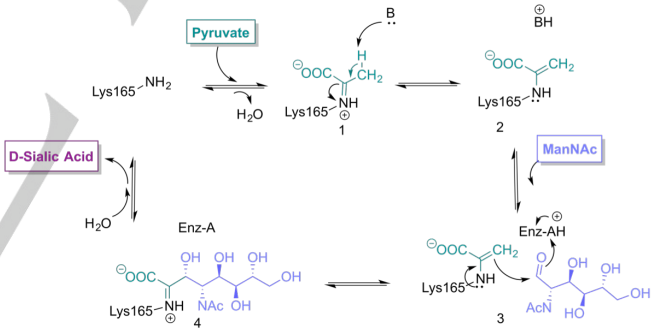


**Scheme 1.** General sequential Bi-Uni reaction mechanism of D-sialic acid aldolase.

Many different crystallographic structures have been reported that contain pyruvate,[6] analogues of pyruvate[7] or D-sialic acid,[8] and in the case of the inactive Tyr137Ala variant an imine D-sialic-pyruvate-Lys165 Schiff-base intermediate was observed as a consequence of the reaction of both species during crystallization.[4b] Directed evolution was applied to convert D-sialic acid aldolase into an efficient L-3-deoxy-manno-2-octulosonic acid (L-KDO) aldolase (see figure 1).[2a] As observed in many DE studies,[3a, 9] the final variant (PDB code: 3LCW[2c]) presented eight mutations occurring at distal positions from the active site (the mean distance between the alpha carbon of all mutations and the catalytic Lys165 is *ca.* 21 Å, see figure 1). This evolved variant exhibited a > 1,000-fold improved ratio of the specificity constant ($[k_{cat}/K_M$(L-KDO)]/[$k_{cat}/K_M$(D-sialic acid)]). Several crystal structures of L-KDO aldolase (8 mutations

[a] A. Romero-Rivera, Dr. J. Iglesias-Fernández, and Prof. S. Osuna
Institut de Química Computacional i Catàlisi (IQCC) and Departament de Química, Universitat de Girona, Carrer Maria Aurèlia Capmany 69, 17003 Girona, Spain.
[b] Catalan Institution for Research and Advanced Studies (ICREA), Passeig Lluïs Companys, 23, 08010, Barcelona, Spain.
e-mail: silvia.osuna@udg.edu, jiglesiasfrn@gmail.com
Webpage: http://iqcc.udg.edu/wordpress/portfolio/silvia-osuna/

Supporting information for this article is given via a link at the end of the document.

including Val251), singly mutated variants (V251I, V251L, V251R, V251W), and the doubly mutated V251I/V265I enzyme were obtained.[2c] Interestingly, mutation of position 251 located 19 Å from Lys165 was found to be key for accommodating substrates of varying size and still retaining stereoselectivity. Although QM/MM studies have been performed to elucidate the reaction mechanism of D-sialic acid aldolase,[4b] the conformational dynamics of the enzyme (and variants) and how the introduced mutations affect the conformational landscape of the enzyme and its substrate specificity still remain unexplored.

In this paper, we evaluate the conformational dynamics of the natural D-sialic acid aldolase, and the DE-evolved variant that exhibits a high selectivity towards the L-arabinose sugar. Our results indicate that the change in specificity is due to a shift in the population of the conformational states, which present different active site volumes and access tunnels. The key role of position Val251 is also investigated.

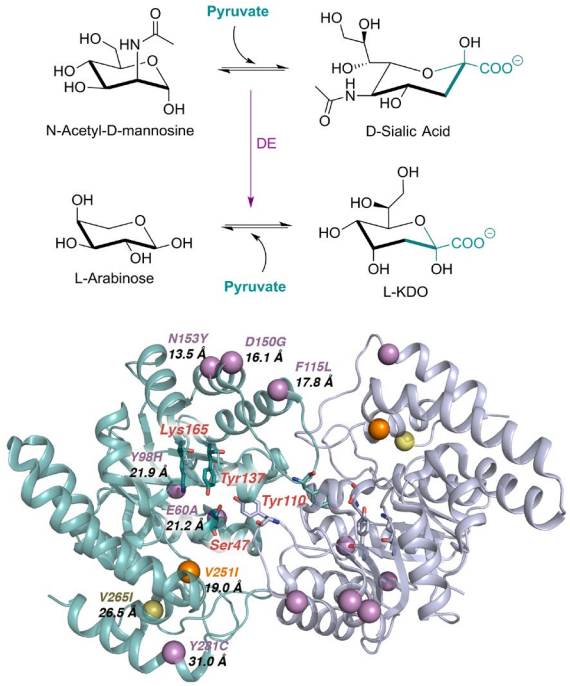


**Figure 1.** a) Directed Evolution of D-sialic acid aldolase to L-KDO aldolase, b) distal mutations introduced shown as spheres together with the distance between the Cα of the mutation and that of catalytic Lys165 (in Å). Among the eight mutations introduced, Val251 (orange) and Val265 (yellow) were found to be key in dictating the specificity of the enzyme.[2c]

## Results and Discussion

*Conformational dynamics of D-sialic acid and L-KDO aldolase*

Our study starts with the evaluation of the conformational dynamics of the natural and evolved variant at the enamine intermediate formed between pyruvate and Lys165 (**2**, see Scheme 1). The crystallographic structure of the L-KDO variant complexed with pyruvate (PDB: 3LCW) was taken as initial structure, whereas for D-sialic acid aldolase pyruvate was docked in the *apo* state crystallographic structure (3LBM, see computational details section). We performed Molecular Dynamics (MD) simulations (i.e an accumulated simulation time of 1.5 microseconds for each system) in explicit water solvent using AMBER.[10] Structural differences along the 1.5 microseconds MD simulations for the D-sialic acid and L-KDO aldolases were analyzed using Principal Component Analysis (PCA) taking into account the distances between pairs of α-carbon residues.

D-sialic acid aldolase explores two main conformational states that are equally populated (see states $\mathbf{1}^{\mathbf{D}}$ and $\mathbf{2}^{\mathbf{D}}$ in figure 2). In $\mathbf{1}^{\mathbf{D}}$, short distances are obtained between the enamine Schiff-base pyruvate intermediate and the catalytic Ser47, and Tyr137 in both active sites (the mean distances are 3.0 ± 0.4 Å, and 4.8 ± 1.6 Å for monomer A, figure 2A). However, Tyr110' from the other subunit is situated at *ca.* 7-9 Å from Tyr137 and Ser47 (figure S2A). The other conformational state $\mathbf{2}^{\mathbf{D}}$ maintains the hydrogen bond network between all catalytic residues Ser47, Tyr137, and Tyr110 (figure 2C) as observed in the X-ray structure. QM/MM studies by Mullholand and Berry showed that lower activation barriers of 6.2-7.7 kcal/mol are obtained when the latter hydrogen bond network takes place.[4b] The $\mathbf{1}^{\mathbf{D}}\rightarrow\mathbf{2}^{\mathbf{D}}$ conversion requires the correct positioning of Tyr110' from *ca.* 7 to *ca.* 3 Å of Ser47. This conformational change of Tyr110' induces a major change in loop L10 (residues 144-148), see movie S1. Interestingly, the latter loop connects the catalytic Tyr137, which is part of a distorted beta sheet (residues 133-138) in monomer A, with alpha-helix 6 (residues 149-156) where two of the DE mutations, i.e. N153Y and D150G, are located.

L-KDO aldolase also displays two main conformational states that are equally populated in solution (see $\mathbf{1}^{\mathbf{L}}$ and $\mathbf{2}^{\mathbf{L}}$ in figure 2B). In $\mathbf{1}^{\mathbf{L}}$, Tyr110'$^{A}$ and Tyr110'$^{B}$ are completely displaced from the active site (at *ca.* 11 Å of Ser47) and are hydrogen bonded at the subunit interface. However, Ser47 and Tyr137 stay close to the enamine Schiff-base pyruvate intermediate in both active sites. The importance of Tyr110' for the catalytic activity of the enzyme was evaluated by Mullholand and Berry.[4b] The mutation of Tyr110 to alanine resulted in a 40-fold decrease of activity, however activity was retained after mutation to the bulkier phenylalanine suggesting that the steric bulk of the residue is important for maintaining Ser47 close to Tyr137. Even though Tyr110' is distal to Ser47 in $\mathbf{1}^{\mathbf{L}}$, both Ser47 and Tyr137 are situated close to the enamine Schiff-base pyruvate intermediate. In conformational state $\mathbf{2}^{\mathbf{L}}$, Tyr110'$^{A}$ and Tyr110'$^{B}$ are situated closer to the active site residues with a distance of *ca.* 5 Å of Ser47. Short distances are also observed between pyruvate and both Ser47 and Tyr137 (figure 2B, D and S2B, D).

Our MD simulations indicate that D-sialic acid and L-KDO aldolases display quite different conformational states, which might be responsible for their different specificity constant towards N-acetyl-D-mannosamine (ManNAc) and L-arabinose.

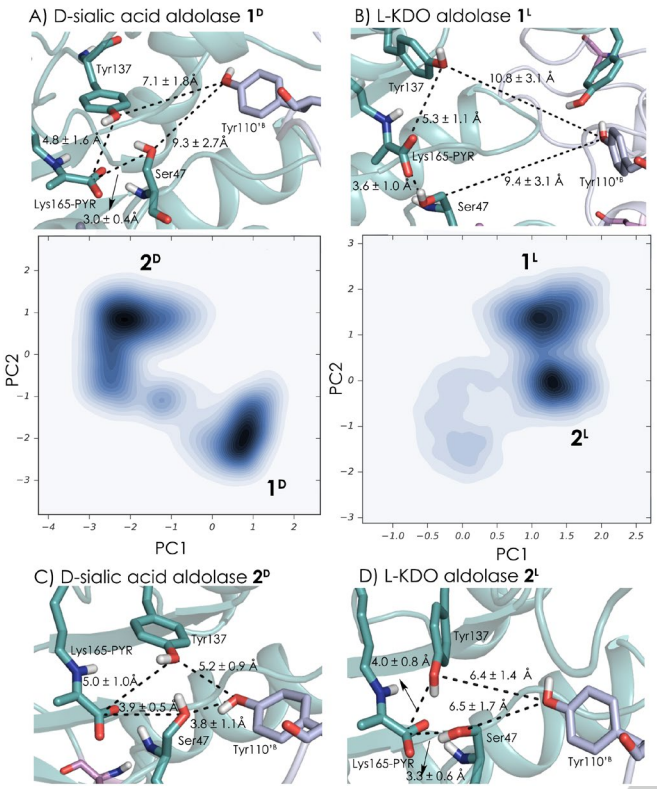


**Figure 2.** Representative snapshots of the active site of D-sialic acid aldolase (A, **1**$^{D}$ and C, **2**$^{D}$) and L-KDO aldolase (B, **1**$^{L}$ and D, **2**$^{L}$) for monomer A. Molecular Dynamics simulations projected onto the two principal components (PC1, PC2) based on the principal component analysis of Cα distances for D-sialic acid aldolase (left, **1**$^{D}$ and **2**$^{D}$) and L-KDO aldolase (right, **1**$^{L}$ and **2**$^{L}$). Mutated residues (pink) and catalytic residues (green and blue) are represented.

*Substrate access tunnels of D-sialic acid and L-KDO aldolase*

The mutations introduced via DE induce a shift in the conformational states that exist in solution for the engineered aldolase, as compared to the WT enzyme (D-sialic acid aldolase). To elucidate the reasons for the experimentally observed change in specificity, we have evaluated the active site shape, as well as substrate access tunnels of the different conformational states sampled by both enzymes. The CAVER 3.0 software[11] was used to compute active site tunnels (see figure 3).

Evaluation of the principal substrate access tunnel for the conformational state **1**$^{D}$ of D-sialic acid aldolase indicates that the displacement of Tyr110' results in a wider active site, with a bottleneck radius of 3.5 ± 0.5 Å and 2.9 ± 0.3 Å for monomer A and B, respectively (figure 3A and S3A). The access tunnel is slightly narrower in **2**$^{D}$ when Tyr110' is properly positioned in the active site (bottleneck radius is 3.4 ± 0.4 Å and 2.2 ± 0.5 Å for monomers A and B, respectively, figure 3C and S3C). As shown in figure 3, Val251 is close to the narrow region of the substrate access tunnel (i.e. the bottleneck). Amino acid changes at position 251 modulate the bottleneck radius of the access tunnel, thus affecting the substrate specificity of the enzyme. Indeed, singly mutated variants at position 251 were found to accommodate substrates of varying size, while still retaining stereoselectivity.[2c]

L-KDO aldolase conformational state **1**$^{L}$ presents both Tyr110'$^{A}$ and Tyr110'$^{B}$ hydrogen bonded, and far away from their respective active sites. Tyr110' conformational change also involves loop L10 (residues 144-148), which in turn modify the active site shape and substrate access tunnel. Computed bottleneck radius for L-KDO monomer A and B are 2.2 ± 0.4 Å and 2.1 ± 0.3 Å, respectively (figure 3B and S3B). Conformational state **2**$^{L}$ presents both Tyr110' close to L-KDO active site residues, and presents a bottleneck radius of 2.3 ± 0.3 Å and 1.9 ± 0.3 Å for monomer A and B, respectively (figure 3D and S3D).

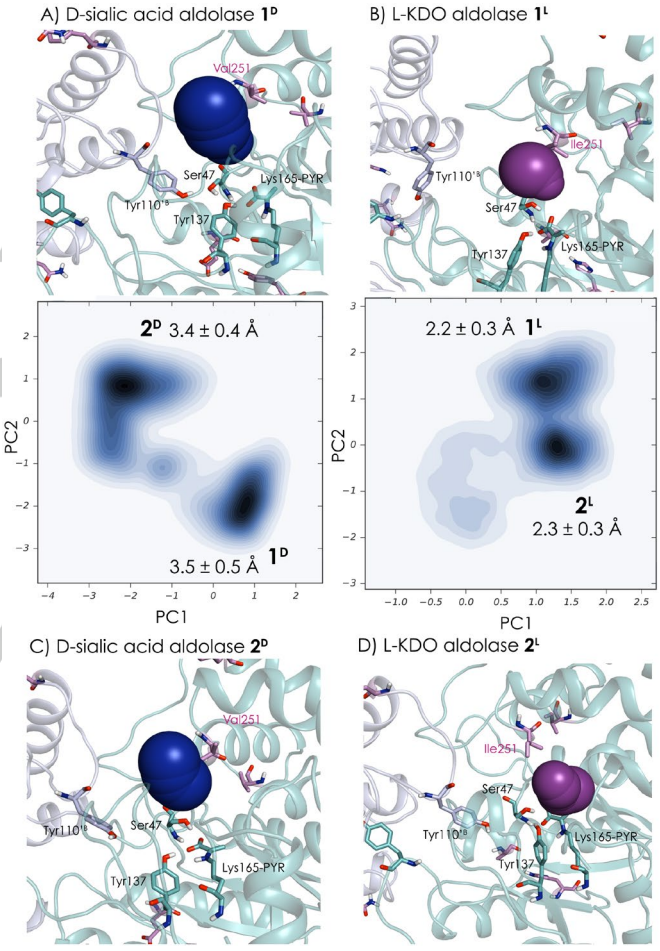


**Figure 3.** Representation of the substrate access tunnels on different representative conformational states that exist in solution for D-sialic acid aldolase (a) and L-KDO aldolase (b) for both monomers. The mean value of the bottleneck radii (in Å) together with the standard deviation is shown. Key mutations located close to the bottleneck of the channel are shown in pink. Catalytic residues (green and blue) are also represented. The same principal components of figure 2 are used to analyse the substrate access tunnels.

Previous structural comparisons of static X-ray structures from D-sialic acid and L-KDO aldolases showed a narrower sugar-binding pocket for the DE variant.[2c] Thanks to our MD simulations

coupled to active site analysis with CAVER we indeed confirm that L-KDO variant explores conformational states that present substrate access tunnels substantially narrower thus restricting its substrate accessibility to small substrates. These differences in the active site shape and accessibility arise from changes in the conformational landscape of the enzyme due to the introduced mutations, and are the main contributing factor to the altered enzyme specificity.

*Substrate binding in D-sialic acid and L-KDO aldolase*

To further confirm the hypothesis of enzyme active site accessibility as the main factor driving substrate specificity, we computed the substrate binding pathway and energy profile with the CAVERDOCK software.[11] As shown in figure 4 for the D-sialic acid aldolase the natural substrate ManNAc binds more tightly to the active site than L-arabinose with an energy difference of approximately 1.3 kcal/mol (figure 5). This more favourable binding energy is in agreement with the smaller $K_M$ values reported experimentally for the reaction with ManNAc as compared to L-arabinose.[2c] Ser208 makes a hydrogen bond with the amide group of ManNAc and contributes to the proper positioning of the natural substrate in the wide active site (figure 4A).

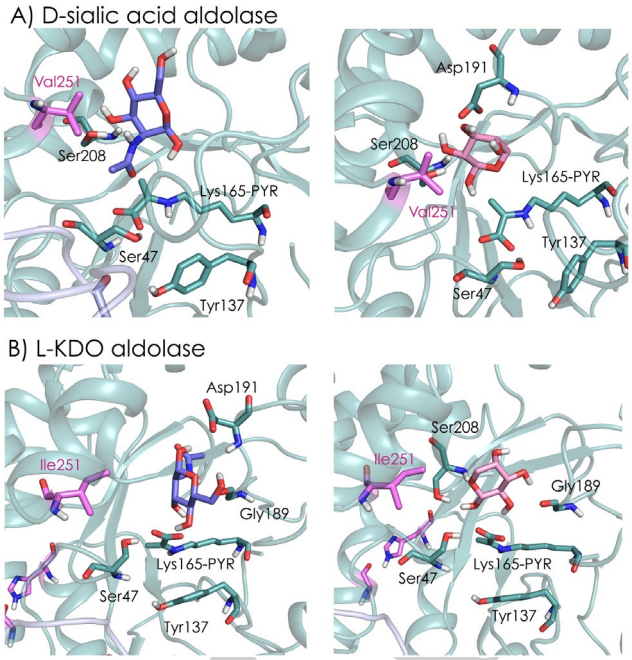


**Figure 4.** Representation of the most relevant hydrogen bond interactions of D-sialic acid (A) and L-KDO (B) aldolases with the docked ManNAc (in lightblue) and L-arabinose (in lightpink) substrates. Mutated residues (pink) and catalytic residues and binding residues (green) are represented.

L-KDO variant shows statistically identical values of the $K_M$ parameters for both substrates, in agreement with the computed energy difference of only 0.3 kcal/mol. It is worth mentioning that for the evolved variant the natural substrate ManNAc is not able to completely access the active site as a consequence of the reduced size and narrower bottleneck radius of the access channel, thus explaining its preferred selectivity towards the smaller L-arabinose. The mutation Val251Ile in L-KDO variant forces the ring of L-arabinose to adopt a different conformation, due the decreased size of the bottleneck. This allows the sugar to interact with Ser208, thus slightly decreasing the binding energy.

The first step in the aldol reaction is the ring-opening of sugar substrates that was proposed to occur in the enzyme active site, which favors the linear open form.[8] Energy profiles computed for the open-ring sugars using the same methodology also match the experimentally reported catalytic activities. Open-ManNAc displays a more favorable binding energy in D-sialic acid aldolase as compared to open-L-arabinose, as a result of the large number of interactions formed that position the substrate for catalysis (figure S5). This is in agreement with the higher $k_{cat}$ of the natural enzyme towards ManNAc. Calculations also indicate that the linear form of the sugar structures is not affected by the narrow L-KDO aldolase tunnel, as both open-L-arabinose and open-ManNAc molecules can access the active site. In this case, specificity of L-KDO aldolase towards L-arabinose can be explained by the higher stability of the later, by approximately 0.5 kcal/mol (figure 5).

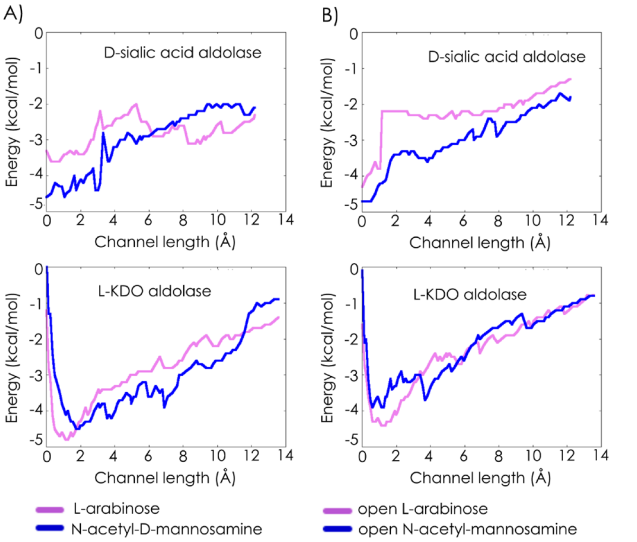


**Figure 5.** Binding energies of the cyclic sugar substrates (A) and open-substrates (B) through the access channel in both enzymes. The active site is located at 0 Å, whereas values of 12-14 Å indicate the outside of the active site. Binding energies for L-arabinose and ManNAc are shown in pink, and blue, respectively.

## Conclusions

Our microsecond MD simulations on the natural D-sialic acid aldolase and the laboratory-engineered L-KDO aldolase that contains eight distal active site mutations, reveal dramatic changes in the enzyme conformational landscape. For D-sialic acid aldolase, the conformational states sampled involve short displacements of Tyr110', This residue was previously described to be important for properly positioning the catalytic Ser47 close

to the Schiff-base intermediate.[4b] In L-KDO aldolase, Tyr110' from both monomers can be completely displaced from the active site and form a hydrogen bond at the dimer interface. It is worth mentioning that Tyr110 connects the loop containing the catalytic Tyr137 and α-helix 6, which define the active site pocket of the enzyme. Thus, its conformational plasticity can be an important factor for modulating the substrate specificity of the enzyme. To further validate our hypothesis of conformational dynamics being a key player in the relaxed specificity of L-KDO aldolase, we analyzed the shape of the enzyme pocket and accessibility. Tunnel calculations done with the CAVER software on the conformational states sampled by both enzymes indicate dramatic changes in the shape and bottleneck radius of substrate access channels, with differences of approximately 1 Å between variants. Narrow bottleneck radii were found for the evolved variant in agreement with its preference towards small substrates. Energy profiles and binding trajectories also confirm the substrate specificity of L-KDO aldolase.

We demonstrate through the combination of Molecular Dynamics (MD) simulations, and in-depth analysis of the active site pocket with the computational tools CAVER and CAVERDOCK, that the effect of distal active site mutations on the enzyme specificity can be rationalized. The understanding of how remote mutations modulate the catalytic properties of enzymes is crucial for the development of more efficient enzyme design protocols. This work describes an efficient strategy for identifying which residues distal to the active site may potentially influence the substrate access to the enzyme active site and thus its specificity.

## Computational details

Molecular Dynamics simulations of the wild-type (PDB 3LBM) and the variant enzyme (PDB 3LCW) in explicit water were performed using the AMBER 16 package.[10] Amber 99SB force field (ff99SB) was used, and parameters for the Lys165-HYD were generated using the general AMBER force field (*gaff*),[12] with partial charges set to fit the electrostatic potential generated at the B3LYP/6-31G(d) level by the restrained electrostatic potential (RESP) model.[13] Amino acid protonation states were predicted using the H++ server (http://biophysics.cs.vt.edu/H++). Water molecules were treated using the SHAKE algorithm, and long-range electrostatic effects were considered using the particle mesh Ewald method.[14] The Langevin equilibration scheme was used to control and equalize the temperature with a 2 fs time step at a constant pressure of 1 atm and temperature of 300 K, and an 8 Å cutoff was applied to Lennard–Jones and electrostatic interactions. Production trajectories were accumulated for 1500 ns, and were analyzed using the *cpptraj* module included in the AMBER 16 package. PCA analysis was done with the *pyEMMA* software.[15]

Substrate access tunnels were analysed using the standalone version of Caver 3.[11] 100 snapshots were randomly selected for each conformational state of D-sialic acid and L-KDO aldolases coming from the 1.5 microseconds MD simulations. The starting point for the channel calculations was selected based on a surface representation of a representative structure of each enzyme (most populated cluster of the 1.5 microsecond MD simulation) with the VMD software[16] (figure S3). Transport tunnels were identified using a probe radius of 0.9 Å. Redundant tunnels were automatically removed from each structure, and the remaining tunnels were clustered using a threshold of 12.

CAVERDOCK a modified version of the AutoDock Vina molecular docking algorithm,[17] was used to compute the substrate binding pathway and energy profile along access tunnels. A single enzyme structure for the D-sialic and L-KDO aldolases was used for the calculations, based on the most populated clustered conformation from a 1μs MD simulation. Access tunnels were calculated with the CAVER 3.0 software as detailed before. The most probable tunnel was discretized to a set of discs, evenly cutting the tunnel. ManNAc and L-arabinose substrates in linear and cyclic forms were used as ligands. CAVERDOCK performs a constrained docking to search for a conformation in the vicinity of the previous docking structure, setting the maximal allowed movement between conformations to 0.8 Å. Energy profiles and docked structures were extracted from the PDBQT output files.

## Acknowledgements

A.R.R. thanks the Generalitat de Catalunya for PhD fellowship (2015-FI-B-00165), J.I.F. is grateful to the European Community for Marie Curie fellowship (H2020-MSCA-IF-2016-753045), S.O. thanks the Spanish MINECO CTQ2014-59212-P, Ramón y Cajal contract (RYC-2014-16846), the European Community for CIG project (PCIG14-GA-2013-630978), and the funding from the European Research Council (ERC) under the European Union's Horizon 2020 research and innovation programme (ERC-2015-StG-679001). We are grateful for the computer resources, technical expertise, and assistance provided by the Barcelona Supercomputing Center - Centro Nacional de Supercomputación.

**Keywords:** aldolase• Molecular Dynamics • substrate access channels • CAVER • conformational dynamics

[1] a) A. Bolt, A. Berry, A. Nelson, *Arch. Biochem. Biophys.* **2008**, *474*, 318-330; b) P. Clapes, W. D. Fessner, G. A. Sprenger, A. K. Samland, *Curr. Opin. Chem. Biol.* **2010**, *14*, 154-167; c) S. M. Dean, W. A. Greenberg, C. H. Wong, *Adv. Synth. Catal.* **2007**, *349*, 1308-1320; d) K. Fesko, M. Gruber-Khadjawi, *Chemcatchem* **2013**, *5*, 1248-1272.

[2] a) C.-C. Hsu, Z. Hong, M. Wada, D. Franke, C.-H. Wong, *Proc. Natl. Acad. Sci. U.S.A.* **2005**, *102*, 9122-9126; b) D. Güclü, A. Szekrenyi, X. Garrabou, M. Kickstein, S. Junker, P. Clapés, W.-D. Fessner, *ACS Catal.* **2016**, *6*, 1848-1852; c) C.-Y. Chou, T.-P. Ko, K.-J. Wu, K.-F. Huang, C.-H. Lin, C.-H. Wong, A. H.-J. Wang, *J. Biol. Chem.* **2011**, *286*, 14057-14064.

[3] a) R. Obexer, S. Studer, L. Giger, D. M. Pinkas, M. G. Gruetter, D. Baker, D. Hilvert, *Chemcatchem* **2014**, *6*, 1043-1050; b) G. Kiss, N. Çelebi-Ölçüm, R. Moretti, D. Baker, K. N. Houk, *Angew. Chem. Int. Ed.* **2013**, *52*, 5700-5725; c) L. Jiang, E. A. Althoff, F. R. Clemente, L. Doyle, D. Röthlisberger, A. Zanghellini, J. L. Gallaher, J. L. Betker, F. Tanaka, C. F. Barbas,

D. Hilvert, K. N. Houk, B. L. Stoddard, D. Baker, *Science* **2008**, *319*, 1387-1391; d) R. Obexer, A. Godina, X. Garrabou, P. R. E. Mittl, D. Baker, A. D. Griffiths, D. Hilvert, *Nat. Chem.* **2017**, *9*, 50-56; e) J. K. Lassila, D. Baker, D. Herschlag, *Proc. Natl. Acad. Sci. U.S.A.* **2010**, *107*, 4937-4942; f) X. Garrabou, T. Beck, D. Hilvert, *Angew. Chem. Int. Ed.* **2015**, *54*, 5609-5612.

[4] a) A. Groher, K. Hoelsch, *J. Mol. Catal. B: Enzym.* **2012**, *83*, 1-7; b) A. D. Daniels, I. Campeotto, M. W. van der Kamp, A. H. Bolt, C. H. Trinh, S. E. V. Phillips, A. R. Pearson, A. Nelson, A. J. Mulholland, A. Berry, *ACS Chem. Biol.* **2014**, *9*, 1025-1032.

[5] C. H. Lin, T. Sugai, R. L. Halcomb, Y. Ichikawa, C. H. Wong, *J. Am. Chem. Soc.* **1992**, *114*, 10138-10145.

[6] I. Campeotto, A. H. Bolt, T. A. Harman, C. Dennis, C. H. Trinh, S. E. V. Phillips, A. Nelson, A. R. Pearson, A. Berry, *J. Mol. Biol.* **2010**, *404*, 56-69.

[7] A. C. Joerger, S. Mayer, A. R. Fersht, *Proc. Natl. Acad. Sci.* **2003**, *100*, 5694-5699.

[8] J. A. R. G. Barbosa, B. J. Smith, R. DeGori, H. C. Ooi, S. M. Marcuccio, E. M. Campi, W. R. Jackson, R. Brossmer, M. Sommer, M. C. Lawrence, *J. Mol. Biol.* **2000**, *303*, 405-421.

[9] A. Currin, N. Swainston, P. J. Day, D. B. Kell, *Chem. Soc. Rev.* **2015**, *44*, 1172-1239.

[10] D. A. Case, T. A. Darden, T. E. Cheatham, C. L. Simmerling, J. Wang, R. E. Duke, R. Luo, M. Crowley, R. C. Walker, W. Zhang, K. M. Merz, B. Wang, S. Hayik, A. Roitberg, G. Seabra, I. Kolossváry, K. F. Wong, F. Paesani, J. Vanicek, X. Wu, S. R. Brozell, T. Steinbrecher, H. Gohlke, L. Yang, C. Tan, J. Mongan, V. Hornak, G. Cui, D. H. Mathews, M. G. Seetin, C. Sagui, V. Babin, P. A. Kollman, *AMBER 16, University of California, San Francisco, 2016*.

[11] E. Chovancova, A. Pavelka, P. Benes, O. Strnad, J. Brezovsky, B. Kozlikova, A. Gora, V. Sustr, M. Klvana, P. Medek, L. Biedermannova, J. Sochor, J. Damborsky, *PLOS Comput. Biol.* **2012**, *8*, e1002708.

[12] J. Wang, R. M. Wolf, J. W. Caldwell, P. A. Kollman, D. A. Case, *J. Comput. Chem.* **2004**, *25*, 1157-1174.

[13] C. I. Bayly, P. Cieplak, W. Cornell, P. A. Kollman, *J. Chem. Phys.* **1993**, *97*, 10269-10280.

[14] T. Darden, D. York, L. Pedersen, *J. Chem. Phys.* **1993**, *98*, 10089-10092.

[15] M. K. Scherer, B. Trendelkamp-Schroer, F. Paul, G. Pérez-Hernández, M. Hoffmann, N. Plattner, C. Wehmeyer, J.-H. Prinz, F. Noé, *J. Chem. Theory Comput.* **2015**, *11*, 5525-5542.

[16] W. Humphrey, A. Dalke, K. Schulten, *J. Mol. Graph.* **1996**, *14*, 33-38.

[17] O. Trott, A. J. Olson, *J. Comput. Chem.* **2010**, *31*, 455-461.

**Entry for the Table of Contents** (Please choose one layout)

Layout 1:

FULL PAPER

Text for Table of Contents

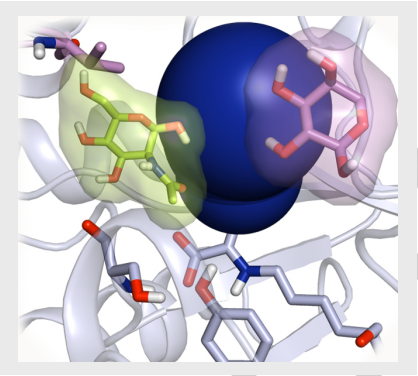

**The analysis of the conformational dynamics of D-sialic acid and L-KDO aldolases reveal a shift in the conformational states sampled by both enzymes. L-KDO aldolase presents a narrower active site and substrate access tunnels, which influence its specificity. The distal mutation I251V plays a key role as it is located at the bottleneck of the substrate access channel.**

*Adrian Romero-Rivera, Javier Iglesias-Fernández,* Sílvia Osuna**

***Page No. – Page No.***

**Exploring the conversion of a D-sialic acid aldolase into a L-KDO aldolase**

Layout 2:

FULL PAPER

((Insert TOC Graphic here; max. width: 11.5 cm; max. height: 2.5 cm; NOTE: the final letter height should not be less than 2 mm.))

Text for Table of Contents

**Key Topic***

*Author(s), Corresponding Author(s)**

***Page No. – Page No.***

**Title**

*one or two words that highlight the emphasis of the paper or the field of the study